Threshold-Independent QRS Detection Using the Dynamic Plosion Index

A. G. Ramakrishnan, *Senior member, IEEE,* A. P. Prathosh and T. V. Ananthapadmanabha

***Abstract*—Detection of QRS serves as a first step in many automated ECG analysis techniques. Motivated by the strong similarities between the signal structures of an ECG signal and the integrated linear prediction residual (ILPR) of voiced speech, an algorithm proposed earlier for epoch detection from ILPR is extended to the problem of QRS detection. The ECG signal is pre-processed by high-pass filtering to remove the baseline wandering and by half-wave rectification to reduce the ambiguities. The initial estimates of the QRS are iteratively obtained using a non-linear temporal feature, named the dynamic plosion index suitable for detection of transients in a signal. These estimates are further refined to obtain a higher temporal accuracy. Unlike most of the high performance algorithms, this technique does not make use of any threshold or differencing operation. The proposed algorithm is validated on the MIT-BIH database using the standard metrics and its performance is found to be comparable to the state-of-the-art algorithms, despite its threshold independence and simple decision logic.**

***Index Terms*—QRS detection, GCI detection, dynamic plosion index, ECG signal, DPI algorithm, threshold free.**

I. Introduction

Techniques for classification and compression of electrocardiogram (ECG) signals and for the analysis of heart rate variability require the detection of QRS as a first step. Numerous approaches proposed in the literature for QRS detection have been well reviewed and compared in [1]. Almost all the high performance algorithms involve two major steps: (i) transformation of the QRS complex into an impulse-like event through some linear or non-linear processing, (ii) R-peak detection by comparing the features of the transformed signal against adaptive [2], [3] or fixed thresholds or with the use of some heuristic detection logic [4]. Among these, methods based on the first derivative of the ECG signal are often used in real time applications because of their low computational load and lack of need for training and patient specific information [5]. Specifically, derivative based methods proposed by Pan and Tompkins [6], Hamilton and Tompkins [7] and Benitez *et al.* [8], [9] are popular. Wavelet-transform (WT) based techniques as in [10], [11] form another set of popular algorithms.

A G Ramakrishnan and A P Prathosh are with the Department of Electrical Engineering, Indian Institute of Science, Bangalore, India - 560012, (e-mail:ramkiag@ee.iisc.ernet.in, prathoshap@ee.iisc.ernet.in).

T V Ananthapadmanabha is with Voice and Speech Systems, Malleswaram, Bangalore, India- 560003, (e-mail: tva_vss@yahoo.com).

All authors of this paper have contributed equally. The code for the author's implemetation of the proposed algorithm can be obtained at http://mile.ee.iisc.ernet.in/QRS/

For correct detection, a common necessity for most of the algorithms is the determination of the thresholds with which the features such as Hilbert transform of the differentiated ECG [8], zero crossings [12] of the pre-processed ECG, the modulus maxima of the WT at different scales [10] are to be compared. Often, these thresholds, which are critical for a good performance, are determined using some heuristics designed to suit the data. Further, many algorithms use additional rules such as search back methods to handle missed detections [5]. In the review of first derivative based methods in [5], it has been reported that false negatives arise (a) due to low amplitude QRS complexes wherein the feature being compared falls below the threshold, (b) during wide, premature ventricular contractions (PVCs) which have lower slope at the R-peak. These are dealt with using secondary thresholds [5]. The first derivative essentially emphasizes the slope of the signal and hence results in a lower amplitude for PVCs which have a lower slope at the R-peak. Additionally, a small-amplitude noise component with a large slope results in a large-amplitude event in the first derivative based methods, which results in false positives. The WT based techniques in [10], [11] involve multiple thresholds and stages of decision logic.

In this paper, we propose a non-linear signal processing method for QRS detection that does not employ any threshold or derivative operations, while offering a comparable performance. Specifically, motivated by the similarities between the integrated linear prediction residual (ILPR) of voiced speech signal and the ECG, we extend the concepts of an algorithm earlier proposed for extraction of the epoch (the significant instant of excitation of the vocal tract within a pitch period) from ILPR [13], to QRS detection from ECG.

II. Proposed method

The two major steps of the algorithm are: (i) Obtaining the high-pass filtered and half-wave rectified ECG as the pre-processed signal, which we refer to as the HHECG. (ii) Using the dynamic plosion index to locate the immediate next QRS, starting from the location of the current QRS, iteratively.

A. Pre-processing

The first step in most of the QRS detection algorithms is to frequency-limit the ECG signal to suppress the baseline wander, and high-frequency noise. Usually, a band-pass filter between 8 and 20 Hz is used. In the current method, we employ only a high-pass filter (HPF) with cutoff frequency (f_c) at 8 Hz to remove the baseline wander since the presence of

some high-frequency components does not significantly affect the results. The HPF is implemented in the frequency domain using a symmetric raised cosine function between 0 and f_c, defined as follows:

$$H(f) = \begin{cases} [0.5 - 0.5\cos(\pi f/f_c)] & 0 \leq f \leq f_c \\ 1 & fc < f \leq fs/2 \end{cases} \quad (1)$$

This filter has a zero phase response, which obviates the need for any phase delay compensation.

Generally, R-peak is of positive polarity and the negative part in the ECG signal contains no information regarding the R-peak instant. Since the goal of this study is to estimate the instants of R-peaks, high-pass filtered ECG signal is half-wave rectified by retaining only the positive part. This step aids the detection algorithm (to be described later) in picking the correct 'peaks' corresponding to the QRS in the processed ECG signal. Rarely, QRS complex may undergo a polarity reversal as noted in [5]. In that case, the 'peak' corresponding to the S-wave is captured by the algorithm in the initial stage. This happens because, within a cycle, the amplitude of the S-wave is generally the largest in the HHECG, when there is a polarity reversal. However, in the second stage of the algorithm, the estimated peak location is refined to latch on to the R-peak of the corresponding cycle.

B. Proposed feature - dynamic plosion index

1) The Plosion Index: Impulse-like, time-localized events occurring within any signal are referred to as the transients. LPR of a speech signal, closure-burst transitions of stop consonants and R-peaks in the ECG signals are examples of such transients. In a previous study [14], we have defined an instant measure to detect such events. In any signal, the ratio of the peak amplitude in a transient to the average of absolute values over a suitably chosen interval in the neighbourhood of the peak is expected to be high. To quantify this, we define the plosion index (PI) at an instant of interest n_0 for any signal $s[n]$ as

$$PI(n_0, m_1, m_2) = \frac{|s(n_0)|}{s_{avg}(n_0, m_1, m_2)} \quad (2)$$

$$where \quad s_{avg}(n_0, m_1, m_2) = \frac{\sum_{i=n_0+m_1+1}^{i=n_0+m_1+m_2} |s(i)|}{m_2} \quad (3)$$

Being a ratio, the PI is dimensionless and independent of the signal level. The intervals covered by m_1 and m_2 depend on the specific application, and in certain cases, may also precede n_0. The significance of the parameters m_1 and m_2 are described in detail in [14].

To illustrate the utility of the PI, Fig. 1 shows a segment of an ECG record along with the corresponding PI values computed at every sample[1]. The variable m_1 is set to 100, to exclude the samples around the R-peak while computing s_{avg} and m_2 is set at 300 which corresponds to the average interval between two successive R-peaks. The values of m_1 and m_2 used here have been chosen by manual observation for the purpose of illustration. It is seen from Fig. 1 (b) that the PI has large values around R-peaks.

[1]Here, we have used the ECG signal without any pre-processing.

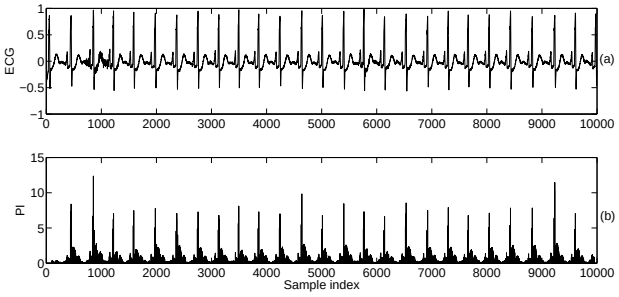

Figure 1. Illustration of the utility of the PI in transient detection, (a) A segment of a normal ECG signal, (b) the corresponding PI values computed on the raw (unprocessed) EEG signal, with $m_1 = 100$ and $m_2 = 300$, respectively. It is seen that the PI has large values around the R-peaks.

2) The dynamic plosion index: To develop an algorithm that does not need any threshold selection, we make use of the dynamic plosion index (DPI) [13]. DPI is the sequence of the values of PI computed at an instant n_0 for N successive values of m_2, with m_1 kept constant. The computation window, discussed in Sec. II.C.2, determines the value of N for this application. The current problem is posed as that of determining the immediate next R-peak given the location of the current R-peak as n_0. The initialization for this process is described later. While computing the DPI with respect to the current R-peak, Eq. (3) is modified as follows.

$$s'_{avg}(n_0, m_1, m_2) = \frac{\sum_{i=n_0+m_1+1}^{i=n_0+m_1+m_2} |s(i)|}{(m_2)^{1/p}}, p > 1 \quad (4)$$

This modification gives a higher weightage to peaks closer to the current peak, to take into account the large dynamics in the amplitudes of R-peaks. This is further clarified during the algorithm description.

The weighted DPI computed (with $p = 2$, $m_1 = -2$) for a segment of HHECG (shown Fig. 2 (a)) of duration 3 s is depicted in Fig. 2 (b). This segment consists of five R-peaks. As m_2 increases past the first reference instant, marked as n_0 in Fig. 2 (a), the DPI gradually increases, reaches a peak and then decreases when m_2 begins to include the signal corresponding to next R-peak. A significant local dip occurs around the immediate next R-peak (around 350^{th} sample). The DPI computed for the next computation window with reference to the next R-peak (marked as n_1 in Fig. 2 (a)) also shows a similar behaviour (depicted with dashed line). We use this nature of the DPI to locate the R-waves.

C. The QRS detection algorithm

1) Initialization : As already mentioned, the problem is posed as that of locating the immediate next R-peak given the location of the current one. This demands a knowledge of the current R-peak at every stage. The proposed algorithm is

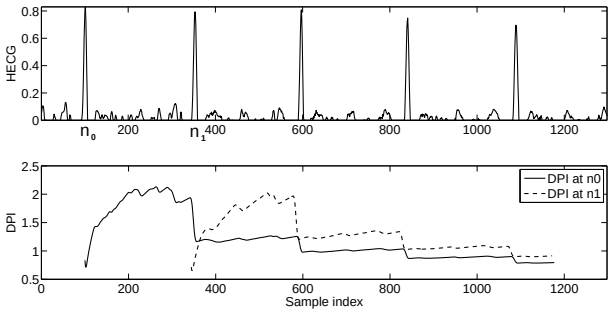

Figure 2. Illustration of the process of locating the next R-peak given the current R-peak using the DPI. (a) HHECG of a segment of ECG signal, (b) The DPI computed with reference to n_0 (solid line) and n_1 (dashed line) on the signal shown in Fig. 2 (a).

insensitive to the initialization for the very first R-peak which is done arbitrarily. The reference instants get automatically aligned to the successive R-peaks within a maximum of three cardiac cycles.

2) DPI algorithm - locating the successive R-peaks: Assuming that the lowest possible heart-rate is 35 BPM, which corresponds to an R-R interval of about 1.71 s, m_2 is varied over a range corresponding to the interval of 0 to 1800 ms (computation window). The variable m_1 is chosen to be -2, to ensure that the $s_{avg}^{'}$ computation includes the current R-peak. Having known the current R-peak, the immediately next R-peak is located using the algorithm described below.

- The DPI of the HHECG is computed over the computation window, with reference to the current R-peak.
- Every pair of successive peaks and valleys in the DPI is noted by detecting the positive and negative zero-crossings in its derivative, respectively.
- The absolute difference (called 'swing') between the values of the DPI at each peak-valley pair is computed.
- From Figs. 2 (a) and (b), it is clear that the peak-valley pair with the largest 'swing' corresponds to the immediate next R-peak. The time instant corresponding to such a valley is noted as the initial estimate.

Usually, the 'swing' corresponding to the immediately next R-peak is the largest. However, at times, due to the large amplitude differences in the R-peaks within a computation window, this may not be the case. This is taken care of by the factor p in the computation of $s_{avg}^{'}$, which non-linearly scales the variable m_2, so that the earlier peaks in the HHECG are given more emphasis than the latter ones.

- Now, the instant of the absolute maximum in the H2ECG signal (described below) within a search interval of the initial estimate is declared as the actual location of the R-peak. The length of the search interval is $\pm$285 ms corresponding to the period of the highest possible heart rate (assumed to be 210 BPM here).

The H2ECG is the ECG signal high-pass filtered locally, within the computation window using Eq. 1 with an f_c of 2 Hz and without any rectification. This removes the local DC-bias within the window and ensures that the correct R-peak is detected even if there is polarity reversal in the QRS. In such cases, the initial estimate from HHECG is the S peak, which is refined to the actual R-peak from the H2ECG signal.

The above procedure is repeated over the entire ECG signal. To illustrate the effectiveness of the algorithm, we depict in Fig. 3, a segment of ECG taken from the record 108 of the MIT-BIH database [15], [16], which is considered noisy. The R-peaks detected for this segment using the DPI algorithm are also overlaid (upward arrows). It is seen that the DPI algorithm has correctly detected the R-peaks, despite the presence of polarity reversal, noise and large baseline wander.

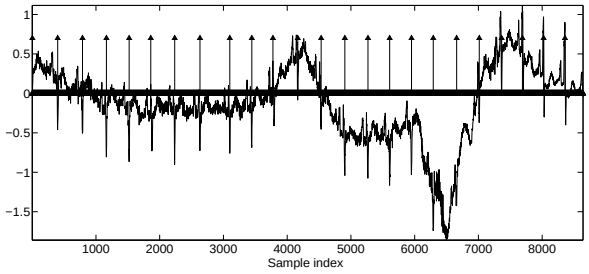

Figure 3. Illustration of the effectiveness of the DPI algorithm on a difficult case from record 108 of MIT-BIH database. A segment of ECG signal is shown (solid line), along with the estimated instants of QRS (upward arrows). The correct R-peaks have been identified in spite of polarity reversal.

III. Evaluation

A. The database and the performance measures

To validate the DPI algorithm, we use the standard MIT-BIH Arrhythmia Database [15], [16]. This contains 48 half-hour sessions of two-channel ambulatory ECG recordings, obtained from 47 subjects. These are digitized at a sampling frequency of 360 Hz using 11 bits over a 10 mV dynamic range.

The algorithm is evaluated using the standard beat-by-beat comparison procedure given in [17], on the first channel of each record. The number of true positives (TP), false positives (FP) and false negatives (FN) are counted for each record leaving out the first five minutes of data deemed as the learning period[2]. The performance measures used are the sensitivity (Se), positive predictivity (+P) and the average time error between the actual and detected peaks as defined in [5]. Similar to the previous studies, the episodes of ventricular flutter occurring in record 207 are excluded from validation.

B. Results

The value of the parameter p used in computing the DPI only marginally affects the performance. Table I lists the values of Se and +P obtained for different values of p. As p increases, Se gradually increases while +P decreases, while both of them remain above 99%. This is expected because, Se depends on FNs, and as p increases, more and more emphasis is given to samples near the current R-peak while computing the DPI. For example, assume that there are three R-peaks R_1, R_2 and R_3 within a computation window, with R_1 being the

[2]The DPI algorithm does not need any learning. However, we excluded the first five minutes of data from validation for fair comparison with other techniques.

current R-peak. If the amplitude of R_2 is significantly lower than that of R_3, there is a chance of 'swing' corresponding to R_3 being higher than that of R_2 thereby missing R_2. In such a case, a higher value of p emphasizes R_2 over R_3, ensuring the 'swing' of R_2 to be greater than that of R_3, which avoids a FN at R_2. A similar but reverse argument may be made regarding decreasing +P with p, since +P depends on FPs.

Table I
PERFORMANCE OF THE DPI ALGORITHM FOR DIFFERENT VALUES OF THE PARAMETER p ON THE ENTIRE MIT-BIH DATABASE.

p	2	3	4	5	6	7	8
Se (%)	99.28	99.44	99.49	99.52	99.53	99.53	99.54
+P (%)	99.83	99.79	99.73	99.70	99.66	99.63	99.59

Table II compares the results for the entire database for $p = 5$, with those of the algorithms reviewed in [5] and [10]. m_e and σ_e represent, respectively, the mean and standard deviation of the timing error made by the algorithm.

Table II
RESULTS OF THE DPI ALGORITHM ON THE ENTIRE MIT-BIH DATABASE COMPARED WITH THOSE OF THE ALGORITHMS REVIEWED IN [5], [10].

Method	Se (%)	+P (%)	m_e (ms)	σ_e (ms)
DPI	99.52	99.70	3.6	6.3
Hamilton-Tompkins (HT)	99.68	99.63	55.82	20.2
Modified HT	99.57	99.59	7.9	4.9
Hilbert Transform (ht)	99.13	99.31	7	8.1
Modified ht	99.29	99.24	7.08	8.1
WT-based	99.80	99.86	-	-

C. Discussion

It may be inferred from Table II that Se and +P of the DPI algorithm are comparable to those of other methods. However, the DPI algorithm offers the least timing error at 3.6 ms. Whereas the algorithms employing thresholds often miss beats in QRS with very low absolute amplitudes, the DPI algorithm rarely misses them. As an example, we illustrate a sample from record 208, along with the detected R-peaks, in Fig. 4. In this segment, there are wide PVCs (e.g., around sample numbers 1750, 2400 and 3000) and very low amplitude R-peaks (between sample numbers 3200 and 4200), in spite of which the DPI algorithm picks up the true R-peaks.

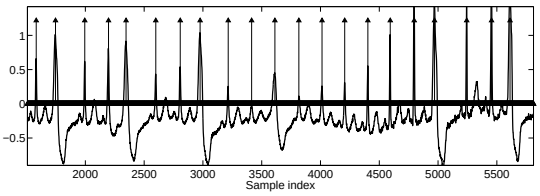

Figure 4. An illustration of the results of the DPI algorithm on a segment with very low-amplitude R-peaks and PVCs. Detected R-peaks are shown by upward arrows.

Although WT-based methods [10], [11] report the highest performance in terms of Se and +P values, they involve multiple blocks of computation and decision logic for detecting every R-peak, which are as follows: (i) four stages of FIR filtering for wavelet decomposition, (ii) computing RMS-like parameters at each scale to determine the threshold with which the respective modulus maxima are to be compared, (iii) computing the regularity exponent at each scale to discard the spurious maxima, (iv) elimination of isolated and redundant modulus maxima using duration and amplitude thresholds, (v) the search-back methods. In contrast, the DPI algorithm involves one filtering and simple selection rules based on maximum values (of swings of DPI for initial estimate and of H2ECG for refinement), for each R-peak detection. Given the aforementioned results, it may be concluded that the DPI algorithm offers significant performance in spite of its threshold independence and simple decision criteria.

D. Cases of failure

The FPs from the DPI algorithm are observed to arise in two situations: (i) when there are QRS-like isolated peaks due to a low signal-to-noise ratio (examples of such cases are seen in record 108), (ii) when the R-R interval is more than the length of the computation window (1.8 s), e.g., some R-peaks in the record 232. This happens due to the presence of episodes of long, non-conducted P-waves in between two successive R-peaks. Based on the DPI formulation, the algorithm hypothesizes at least one QRS within each computation window. Thus for records with very long R-R intervals, the DPI algorithm places false positives between the true R-peaks.

The only observed case of FN is when there is a very low-amplitude R-peak sandwiched between two very large-amplitude R-peaks. In the DPI computed on a segment of ECG signal with such a pattern, the 'swing' due to the smaller amplitude R-peak is lower than that of the following R-peak. This causes the algorithm to miss such a beat. Examples of such cases may be seen around 500 seconds in record 228, where small amplitude normal beats are interspersed between two large amplitude PVCs.

IV. CONCLUSION

In this paper, we have proposed the DPI algorithm for QRS detection. The high-pass filtered ECG signal is half wave rectified in the pre-processing stage. A new temporal measure, the plosion index, proposed earlier to detect 'transients' in signals, has been used. An extension of the PI, called the dynamic plosion index has been applied on the pre-processed signal to detect the R-peaks, which avoids the use of any threshold and differencing operation. Further, the proposed method detects the QRS even (a) when there is a polarity reversal, (b) when the R-peaks are of very low amplitude and (c) within cycles containing wide premature ventricular contractions. The DPI algorithm has been validated using the standard procedures against the MIT-BIH database and the performance is comparable to the best reported in the literature. Since the WT-based methods have been used for telemonitoring applications [18], in our future work, we intend to explore the applicability of the DPI algorithm for similar applications.

REFERENCES

[1] B. U. Kohler, C. Hennig, and R. Orglmeister, "The principles of software QRS detection," *IEEE Eng. Med. Biol. Mag*, vol. 21, no.1, pp. 42–57, 2002.

[2] I. Christov, "Real time electrocardiogram QRS detection using combined adaptive threshold," *Biomed. Eng. Online*, vol. 3, no. 28, 2004.

[3] J. Lewandowski, H. E. Arochena, R. N. G. Naguib, and K.-M. Chao, "A simple real-time QRS detection algorithm utilizing curve-length concept with combined adaptive threshold for electrocardiogram signal classification," in *Proc.TENCON 2012 - IEEE Region 10 Conference*, Cebu, Nov. 2012, pp. 1–6.

[4] V. X. Afonso, W. J. Tompkins, T. Q. Nguyen, and S. Luo, "ECG beat detection using filter banks," *IEEE Trans. Biomed. Eng*, vol. 46, no.2, pp. 192–202, Feb. 1999.

[5] N. M. Arzenoa, Z.-D. Deng, and C.-S. Poon, "Analysis of first-derivative based QRS detection algorithms," *IEEE Trans. Biomed. Eng*, vol. 55, no.2, pp. 478–484, Feb. 2008.

[6] J. Pan and W. J. Tompkins, "A real-time QRS detection algorithm," *IEEE Trans. Eng. Biomed. Eng.*, vol. 32, no. 3, pp. 230 – 236, 1985.

[7] P. S. Hamilton and W. J. Tompkins, "Quantitative investigation of QRS detection rules using the MIT/BIH arrhythmia database," *IEEE Trans. Eng. Biomed. Eng.*, vol. 33, no. 12, pp. 1157–1165, 1986.

[8] D. S. Benitez, P. A. Gaydecki, A. Zaidi, and A. P. Fitzpatrick, "A new QRS detection algorithm based on the Hilbert transform," *Comput. Cardiol.*, vol. 27, pp. 379–382, 2000.

[9] D. Benitez, P. Gaydecki, A. Zaidi, and A. Fitzpatrick, "The use of the Hilbert transform in ECG signal analysis," *Comput. Biol. Med.*, vol. 31, pp. 399–406, 2001.

[10] C. Li, C. Zheng, and C. Tai, "Detection of ECG characteristic points using wavelet transforms," *IEEE Trans. Biomed. Eng*, vol. 42, no.1, pp. 21–28, Jan. 1995.

[11] J. P. Martinez, R. Almeida, S. Olmos, A. P. Rocha, and P. Laguna, "A wavelet-based ECG delineator: Evaluation on standard databases," *IEEE Trans. Biomed. Eng*, vol. 51, no.4, pp. 570–581, Apr. 2004.

[12] B. U. Kohler, C. Hennig, and R. Orglmeister, "QRS detection using zero crossing counts," *Progress in Biomedical Research*, vol. 8, no.3, pp. 138–145, 2003.

[13] A. P. Prathosh, T. V. Ananthapadmanabha, and A. G. Ramakrishnan, "Epoch extraction based on integrated linear prediction residual using plosion index," *IEEE Trans. on Audio, Speech, and Lang. Process.*, vol. 21, no-12, pp. 2471–2480, Dec. 2013.

[14] T. V. Ananthapadmanabha, A. P. Prathosh, and A. G. Ramakrishnan, "Detection of the closure-burst transitions of stops and affricates in continuous speech using the plosion index," *J. Acoust. Soc. Amer.*, vol. 135 no.1, pp. 460–471, Jan. 2014.

[15] G. B. Moody and R. G. Mark, "The impact of the MIT-BIH arrhythmia database," *IEEE Eng. in Med. and Biol.*, vol. 20, no. 3, pp. 45–50, 2001.

[16] A. L. Goldberger, L. A. Amaral, L. Glass, J. M. Hausdorff, P. C. Ivanov, R. G. Mark, J. E. Mietus, G. B. Moody, C. K. Peng, and H. E. Stanley, "Physiobank, Physiotoolkit, and Physionet: Components of a new research resource for complex physiologic signals," *Circulation*, vol. 101, no. 23, pp. e215–e220, 2000.

[17] Association for the Advancement of Medical Instrumentation, "Testing and reporting performance results of cardiac rhythm and ST segment measurement algorithms," *ANSI/AAMI/ISO EC57:1998/(R)2008*, pp. 1–36, 2008.

[18] F. Rincon, J. Recas, N. Khaled, and D. Atienza, "Development and evaluation of multilead wavelet-based ECG delineation algorithms for embedded wireless sensor nodes," *IEEE Trans.Information Technology in Biomedicine*, vol. 15, no.6, pp. 854–863, Nov. 2011.